A Multiclass Arousal Recognition using HRV Nonlinear Analysis and Affective Images

M. Nardelli[1], A. Greco[1], G. Valenza[1], A. Lanata[1], and R. Bailón[2,3,‡], E.P. Scilingo[1,‡,*]

***Abstract*— This paper reports on a multiclass arousal recognition system based on autonomic nervous system linear and nonlinear dynamics during affective visual elicitation. We propose a new hybrid method based on Lagged Poincaré Plot (LPP) and symbolic analysis, hereinafter called LPP$_{symb}$. This tool uses symbolic analysis to evaluate the irregularity of the trends of Lagged Poincaré Plot (LPP) quantifiers over the lags, and is here applied to investigate complex Heart Rate Variability (HRV) changes during emotion stimuli. In the experimental protocol 22 healthy subjects were elicited through a passive visualization of affective images gathered from the international affective picture system. LPP$_{symb}$ and standard HRV analysis (defined in time and frequency domains) were applied to HRV series of one minute length. Then, an ad-hoc pattern recognition algorithm based on quadratic discriminant classifier was implemented and validated through a leave-one-subject-out procedure. The best performance of the proposed classification algorithm for recognizing the four classes of arousal was obtained using nine features comprising heartbeat complex dynamics, achieving an accuracy of 71.59%.**

I. Introduction

Emotions provide the substrate for most of real life aspects, from social interactions to decision-making processes [1], [2]. The capacity to regulate emotions in agreement with the external context is fundamental for social functioning and for preserving mental health [3], [4]. Different levels of physiological arousal, or alertness, in human body are the results of the interaction between emotion experience and environment changes [5].

The study of emotions has a long history in psychology [6], [7], and has led to the development of several models. One of the most widely used model is the Circumplex Model of Affect (CMA) [8], which represents emotions in a multidimensional space. Arousal (i.e., degree of activation) and valence (i.e., pleasantness/unpleasantness) levels are the two principal dimensions of the CMA [8].

In the literature, physiological changes in response to different kinds of emotional stimuli have been extensively investigated, including affective images [9]–[11] and sounds [12], [13] from standardized databases. Concerning visual elicitation, the International Affective Picture System (IAPS) [9] is one of the mostly used set of stimuli and comprise of 944 images characterized by different values of arousal and valence.

This research has received funding from the European Commission H2020 programme under grant agreement no. 689691 (NEVERMIND).

[1]Department of Information Engineering & Research Centre E. Piaggio, School of Engineering, University of Pisa, Pisa, Italy

[2]BSICoS Group, Aragón Institute of Engineering Research (I3A), IIS Aragón, University of Zaragoza, Zaragoza, Spain

[3]CIBER of Bioengineering, Biomaterials and Nanomedicine (CIBER - BBN), Madrid, Spain

‡ Senior Authors; * Corresponding author,

e-mail: e.scilingo@centropiaggio.unipi.it.

The Autonomic Nervous System (ANS) plays a crucial role in the management of emotions. Particularly, it is known to affect heartbeat dynamics in response to emotional stimuli trough the modulation of the activity of its two branches: the sympathetic and the parasympathetic nervous systems. Indeed, Heart Rate Variability (HRV) linear and nonlinear analyses are now considered an effective means to study changes in ANS dynamics due to stimuli with different arousal and valence levels.

In this context, the Lagged Poincaré Plot (LPP) is a powerful tool for the nonlinear analysis of HRV series. In a previous study [14], we successfully employed LPPs to study cardiovascular dynamics during affective elicitation administered through the International Affective Digitized Sounds. We found that the shape of LPP was influenced by the arousal level associated with acoustic stimuli, and that the differences in magnitute of LPP quantifiers are dependant from both the lags and arousal scores. Concerning the IAPS elicitation, a previous study used LPP metrics to classify four discrete emotions, i.e., happiness, relaxation, sadness, and fear [15]. They concluded that the Poincaré Plot geometrical shapes significantly change as a function of the positive and negative valence of emotions.

Here we apply the LPP_{symb}, a novel hybrid approach combining LPP and Symbolic Analysis [16], to quantify the variability of LPP quantifiers as a function of the lags. We recently tested with success the performance of LPP_{symb} while investigating emotional changes along the valence dimension (i.e., pleasantness vs. unpleasantness) [17]. In that preliminary endeavour we found a significant increase of the variability of LPP shape over the lags associated with pleasant images. Here, LPP_{symb} is employed to study the physiological arousal as elicited by means of IAPS images in healthy subjects. To this extent, we here propose an *ad-hoc* pattern recognition algorithm based on a Quadratic Discriminant Classifier (QDC) and a Leave-One-Subject-Out (LOSO) validation procedure to automatically discriminate four levels of arousal.

II. Materials and Methods

A. Subjects Recruitment, Experimental protocol and Acquisition set-up

Twenty-two healthy volunteers (range 21-24 years old) were involved in the experiment. Participants did not suffer from any cardiovascular, psychological and neurological diseases, and were aware of the purpose of the experiment. The ethical committee of University of Pisa approved all experimental procedures involving human subjects in this study. All subjects were screened using the Patient Health Questionnaire, and only the ones with a score lower than 5

978-1-5386-3646-6/18/$31.00 ©2018 IEEE

were included for further analyses and tests [18]. During the experiment, participants were emotionally elicited through passive visualization of the IAPS pictures onto a PC monitor.

At the beginning of the experiment, subjects were in a resting state for 5 minutes, with their eyes closed. Then, nine sessions of slide-show started: four arousal sessions were interposed between five neutral sessions. One-minute resting-state sessions were in between each neutral and arousal session (see Figure 1 for the experiment timeline). Neutral sessions consisted of 6 images (valence range of 5.52-7.08 and arousal range of 2.42-3.22). The arousal sessions included 20 images with an increasing level of valence (from unpleasant to pleasant), the first and the second arousal had a low-medium (L-M) score of arousal, whereas the images in the last two were chosen in order to be considered with a medium-high (M-H) arousal score. The L-M arousal sessions had a valence range from 1.95 to 8.03, and an arousal range from 3.08 to 4.99. The M-H arousal sessions had a valence range from 1.49 to 7.77, and an arousal range from 5.01 to 6.99. A total of 110 images was shown and each image was presented for 10 seconds.

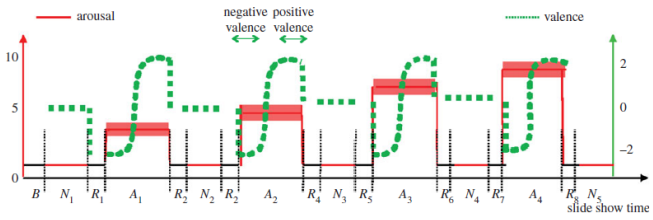

Fig. 1. Experimental timeline. The y-axis relates to the official IAPS score, whereas the x-axis relates to the time. Along time, the red line indicates the arousal level and the dotted green line the valence level. R=rest sessions, N=neutral sessions, A=arousal sessions.

Electrocardiographic (ECG) signals of the participants were acquired throughout the experimental protocol, by means of the ECG100C Electrocardiogram Amplifier from BIOPAC inc., with a sampling rate of 500 Hz. The interbeat series (RR interval series) were extracted using Pan-Tompkins algorithm for peak detection [19]. Artifacts and ectopic beats were corrected through the use of Kubios HRV software [20].

B. Feature extraction

In order to uniform the length of the time series to extract HRV features, we used time-windows with a fixed duration of one minute. Each neutral session lasted one minute, whereas the arousing sessions were divided into two parts according to the two levels of valence (negative and positive) which lasted one minute and half each. Each valence session was split into two windows of one minute each, with an overlap of thirty seconds, then the mean value between the parameters computed in the two windows was considered.

1) Time and Frequency HRV Analysis: Standard HRV features belonging to time and frequency domains were extracted from one-minute HRV series. From RR series we calculated the mean of RR intervals (RR mean), the standard deviation (RR std). Frequency parameters of HRV were obtained from the power spectral density (PSD) of the modulating signal computed using the Integral Pulse Frequency Modulation (IPFM) model [21]. Power Spectral Density (PSD) was estimated using Welch's periodogram and the power values in the LF (from 0.04 to 0.15 Hz) and HF (from 0.15 to 0.4 Hz) bands were calculated, together with their ratio (LF/HF). We also computed the power in the LF and HF band normalized by the total power (LF power% and HF power%, considering the total power in the band from 0 to 0.4 Hz), and, only for LF, by the sum of the LF and HF power (LF power nu). Finally, we calculated the values of the frequencies having maximum magnitude (LF peak and HF peak).

2) LPP_{symb}: as mentioned above, in this study we propose a joint method, called LPP_{symb}, in order to study the trend of the LPP traditional parameters ($SD1$, $SD2$, S, $SD12$). LPP traditional parameters are computed following the ellipse-fitting method, which proposes to fit an imaginary ellipse on the scatterplot and to extract some geometrical parameters from it [22]. Following the LPP method, a scatterplot of the lagged RR interval series, RR_{n+M}, against the series RR_n, is built and M is the lag. LPP traditional descriptors are extracted for each lag:

- SD1: the standard deviation of the points calculated along the direction perpendicular to the line-of-identity $RR_{n+M} = RR_n$;
- SD2: the standard deviation of the points along the line-of-identity $RR_{n+M} = RR_n$;
- SD12 ($SD12 = SD1/SD2$): the ratio between SD1 and SD2;
- S ($S = \pi \times SD1 \times SD2$): the area of an imaginary ellipse with axes SD1 and SD2

In order to describe the trends of all these quantifiers as a function of M, we investigated the symbolic dynamics of the LPP considering a large range of M lag values, from 1 to 30. We divided the amplitude range of each LPP quantifier as a function of M lag in 12 equal levels, and we assigned to each one a symbol from 0 to 11. From the symbolic series of 30 samples, we then constructed patterns of three symbols [16], with a time delay between samples equal to one. Then we counted the number of words with at least one variation in the symbols and we extract the percentage value according to the total number of patterns.
As exploratory study, the same approach was computed adding a dimension to the symbolic patterns (four symbols). In this case, we identified the cases where the four-symbols patterns contain at least two variations. Also in this case the percentage values were computed.
Applying this approach, two features for each LPP parameters can be calculated, one for three symbol patterns and one for four symbol patterns, for a total of 8 features. Concerning the notation employed in this study, we used, for example, $SD2_{LPPS3}$ and $SD2_{LPPS4}$ when the LPP_{symb} is applied to the trend of SD2, considering three symbol words and four symbol words respectively.

C. Pattern Recognition and Statistical Analysis

The HRV features extracted from the experimental series were used to discriminate the four levels of arousal. The number of samples in each class was equal to the number of subjects multiplied by the number of arousal sessions, i.e. 88.

A total of nine repetitions have been computed, increasing the number of dimensions (i.e., features) of the feature-space from 1 to 9. In order to avoid overfitting risk, the maximum number of features (9) was chosen following the well known rule-of-thumb whereby the number of features should be less than the square root of the number of examples of each class [23]. At each repetition, we implemented a LOSO cross-validation procedure, which used a training set of N-1 subjects for model selection and parameter optimization. Concerning the feature selection, we applied a *filter method* [24] based on Friedman non-parametric statistical test between the arousal levels. We selected and ranked the 9 features that presented the lowest p-values. In addition, at each LOSO iteration, the training set was normalized using a non-parametric version of z-score approach. The normalization consisted of two steps: (i) each feature value calculated during the neutral session was subtracted from the corresponding value estimated during the successive arousal session; (ii) the value obtained at the first step was divided by the median absolute deviation (MAD) evaluated over the training set for the considered arousal session. The classifier employed for the pattern recognition was a QDC [23].
In addition, in order to better understand the trend of the features with the increase of the arousal scores, we also applied the Wilcoxon nonparametric statistical test for each feature between the two macro-levels of arousal, i.e., L-M and M-H.

III. Experimental Results

Table I reports the confusion matrix related to the best performance, in terms of accuracy, obtained by the proposed pattern recognition algorithm. Such a maximum accuracy was achieved using the first nine most informative features, therefore avoiding the risk of model overfitting.

TABLE I

PEAK PERFORMANCE OF THE PATTERN RECOGNITION IN THE DISCRIMINATION BETWEEN FOUR DIFFERENT LEVELS OF AROUSAL.

	Arousal 1	**Arousal 2**	**Arousal 3**	**Arousal 4**
Arousal 1	**81.8182**	9.0909	31.8182	9.0909
Arousal 2	4.5455	**77.2727**	18.1818	0.0000
Arousal 3	13.6363	4.4545	**45.4545**	9.0909
Arousal 4	0.0000	9.0909	4.5455	**81.8182**

The highest accuracy was 71.59%, calculated as the mean of values along the diagonal of the confusion matrix (Table I). Table II shows the HRV features selected at least in one LOSO iteration, for a total amount of 14 features (2 in the time-domain, 7 in the frequency domain and 5 derived from LPP_{symb}).

As mentioned in Section II-C, the selection criterion was based on the Friedman non-parametric statistical test among the four arousal sessions. It is worthwhile noting that Friedman test and the correspondent post-hoc analysis showed significant differences between the HF power values calculated in the four sessions (p-value=0.01), with a decreasing trend from the least to the most arousing, and between the values of HF peak (p-value=0.03), with a higher value related to the last three arousal sessions in comparison with the first one. In addition, Wilcoxon nonparametric statistical test was also applied to distinguish L-M from M-H arousal sessions. In Figure 2 the significant results of Wilcoxon test are reported for some of the parameters selected by the algorithm, showing their trend (median and MAD) and the corresponding p-value. We found a significant decrease of HF power when the arousal scores of the images increased (p-value=0.041). Features $SD2_{LPP3}$ and $SD2_{LPP4}$ showed the same trend of RR mean, with a significant increase during more arousing sessions.

TABLE II

FEATURES SELECTED BY THE ALGORITHM AT LEAST IN ONE ITERATION.

STANDARD	LPP_{symb}
LF/HF	$SD2_{LPP4}$
HF peak	$SD2_{LPP3}$
RR mean	S_{LPP4}
LF power nu	$SD1_{LPP3}$
HF power	$SD12_{LPP3}$
RR std	
HF power %	
LF power	
LF power %	

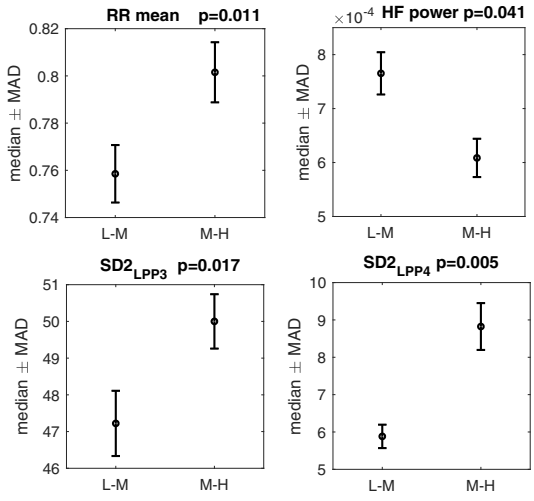

Fig. 2. Wilcoxon test applied to two standard parameters (RR mean and HF power) and to two LPP_{symb} parameters ($SD2_{LPP3}$ and $SD2_{LPP4}$) for discerning L-M from M-H arousal level. The parameters are expressed as median value and median absolute deviation (MAD).

IV. Conclusion and Discussion

In this study we proposed a novel multi-class arousal recognition approach based on the HRV analysis for visual emotional elicitation. All HRV features were extracted from one-minute HRV series from 22 healthy subjects who were emotionally elicited through passive visualization of images gathered from the IAPS database. We implemented standard HRV analysis defined in the time and frequency domains, as well as a hybrid approach (LPP_{symb}) which is derived from two nonlinear analysis methods: LPP and Symbolic Analysis.

LPP technique is a lagged version of Poincaré's return map theory, and it was already used in the literature to investigate autonomic response to acoustic [14], [25] and visual affective stimulation [15], [26]. We have previously suggested LPP_{symb} to quantify the relative peak frequencies in the trends of LPP parameters aiming at evaluating the variability of these quantifiers over the lags. Particularly,

we have used the LPP_{symb} in an application where we classified the valence level of IAPS images [17]. Here we used a pattern recognition approach based on QDC classifiers to recognize four different arousal levels elicited through IAPS images. Note that the same classification procedures including effective feature selection steps were successfully applied in [14], [17].

Experimental results showed that we were able to classify the four arousal sessions reaching a peak of accuracy at 71.59% using nine HRV features only. The third arousal session was the most misclassified (accuracy of 45.45%). Although at a speculation level, this can be explained by the fact that the second and the third sessions had an intermediate arousal level (M-L and M-H) which could have determined a sort of habituation phenomenon, and/or a non optimal differential emotional perception of the user. As expected, the two sessions with lowest and highest arousal level (first and fourth) were associated with the maximum recognition accuracy.

Results from the statistical analysis showed a decrease of the HRV power in the high frequency band, i.e. between 0.15 Hz and 0.4 Hz, going from the lowest level of arousal to the highest (see Figure 2). Note that HF power is known to be associated with the parasympathetic activity [27]. The decrease of parasympathetic activity during arousal stimulation is coherent with the literature reporting on the physiological response to arousing conditions [28]. Likewise, the trends of the LPP_{symb} features selected by the pattern recognition algorithm ($SD2_{LPP4}$ and $SD2_{LPP3}$), were coherent with the image arousal level ($p < 0.01$ for $SD2_{LPP4}$ after Wilcoxon statistical test). As per previous evidences [29], we could speculate that the increase of arousal level leads to an increase of the variability in the length of the Poincaré Plot over the lags, which can be influenced by changes in both high and low frequency components of HRV.

Future studies will focus on investigating the valence modulation effect throughout arousal recognition, also considering other kinds of emotional elicitation (e.g., audio, touch, odours).

REFERENCES

[1] A. R. Damasio, *Looking for Spinoza: Joy, sorrow, and the feeling brain*. Houghton Mifflin Harcourt, 2003.

[2] D. Keltner and A. M. Kring, "Emotion, social function, and psychopathology." *Review of General Psychology*, vol. 2, no. 3, p. 320, 1998.

[3] N. Eisenberg, R. A. Fabes, B. Murphy, P. Maszk, M. Smith, and M. Karbon, "The role of emotionality and regulation in children's social functioning: A longitudinal study," *Child development*, vol. 66, no. 5, pp. 1360–1384, 1995.

[4] J. J. Gross and R. F. Muñoz, "Emotion regulation and mental health," *Clinical psychology: Science and practice*, vol. 2, no. 2, pp. 151–164, 1995.

[5] B. M. Appelhans and L. J. Luecken, "Heart rate variability as an index of regulated emotional responding." *Review of general psychology*, vol. 10, no. 3, p. 229, 2006.

[6] J. A. Russell, "Core affect and the psychological construction of emotion." *Psychological review*, vol. 110, no. 1, p. 145, 2003.

[7] D. Watson, D. Wiese, J. Vaidya, and A. Tellegen, "The two general activation systems of affect: Structural findings, evolutionary considerations, and psychobiological evidence." *Journal of personality and social psychology*, vol. 76, no. 5, p. 820, 1999.

[8] J. Posner, J. A. Russell, and B. S. Peterson, "The circumplex model of affect: An integrative approach to affective neuroscience, cognitive development, and psychopathology," *Development and psychopathology*, vol. 17, no. 3, pp. 715–734, 2005.

[9] P. J. Lang, M. M. Bradley, and B. N. Cuthbert, "International affective picture system (iaps): Affective ratings of pictures and instruction manual," *Technical report A-8*, 2008.

[10] G. Valenza, A. Greco, C. Gentili, A. Lanata, L. Sebastiani, D. Menicucci, A. Gemignani, and E. Scilingo, "Combining electroencephalographic activity and instantaneous heart rate for assessing brain–heart dynamics during visual emotional elicitation in healthy subjects," *Phil. Trans. R. Soc. A*, vol. 374, no. 2067, 2016.

[11] L. Faes, A. Greco, A. Lanata, R. Barbieri, E. P. Scilingo, and G. Valenza, "Causal brain-heart information transfer during visual emotional elicitation in healthy subjects: Preliminary evaluations and future perspectives," in *Engineering in Medicine and Biology Society (EMBC), 2017 39th Annual International Conference of the IEEE*. IEEE, 2017, pp. 1559–1562.

[12] M. M. Bradley and P. J. Lang, "The international affective digitized sounds (; iads-2): Affective ratings of sounds and instruction manual," *University of Florida, Gainesville, FL, Tech. Rep. B-3*, 2007.

[13] A. Greco, G. Valenza, L. Citi, and E. P. Scilingo, "Arousal and valence recognition of affective sounds based on electrodermal activity," *IEEE Sensors Journal*, vol. 17, no. 3, pp. 716–725, 2017.

[14] M. Nardelli, G. Valenza, A. Greco, A. Lanata, and E. P. Scilingo, "Recognizing emotions induced by affective sounds through heart rate variability," *IEEE Transactions on Affective Computing*, vol. 6, no. 4, pp. 385–394, 2015.

[15] A. Goshvarpour, A. Abbasi, and A. Goshvarpour, "Indices from lagged poincare plots of heart rate variability: an efficient nonlinear tool for emotion discrimination," *Australasian Physical & Engineering Sciences in Medicine*, pp. 1–11, 2017.

[16] A. Porta, E. Tobaldini, S. Guzzetti, R. Furlan, N. Montano, and T. Gnecchi-Ruscone, "Assessment of cardiac autonomic modulation during graded head-up tilt by symbolic analysis of heart rate variability." *American journal of physiology. Heart and circulatory physiology*, vol. 293, no. 1, pp. H702–8, 2007.

[17] M. Nardelli, A. Greco, G. Valenza, A. Lanata, R. Bailón, and E. Scilingo, "A novel heart rate variability analysis using lagged poincaré plot: A study on hedonic visual elicitation," in *Engineering in Medicine and Biology Society (EMBC), 2017 39th Annual International Conference of the IEEE*. IEEE, 2017, pp. 2300–2303.

[18] K. Kroenke, R. L. Spitzer, and J. B. Williams, "The patient health questionnaire-2: validity of a two-item depression screener," *Medical care*, vol. 41, no. 11, pp. 1284–1292, 2003.

[19] J. Pan and W. J. Tompkins, "A real-time qrs detection algorithm," *IEEE transactions on biomedical engineering*, no. 3, pp. 230–236, 1985.

[20] M. P. Tarvainen, J.-P. Niskanen, J. A. Lipponen, P. O. Ranta-Aho, and P. A. Karjalainen, "Kubios hrv–heart rate variability analysis software," *Computer methods and programs in biomedicine*, vol. 113, no. 1, pp. 210–220, 2014.

[21] J. Mateo and P. Laguna, "Analysis of heart rate variability in the presence of ectopic beats using the heart timing signal," *IEEE Transactions on Biomedical Engineering*, vol. 50, no. 3, pp. 334–343, 2003.

[22] M. P. Tulppo, T. Makikallio, T. Takala, T. Seppanen, and H. V. Huikuri, "Quantitative beat-to-beat analysis of heart rate dynamics during exercise," *American journal of physiology-heart and circulatory physiology*, vol. 271, no. 1, pp. H244–H252, 1996.

[23] R. O. Duda, P. E. Hart, and D. G. Stork, *Pattern classification*. John Wiley & Sons, 2012.

[24] K. Kira and L. A. Rendell, "A practical approach to feature selection," in *Machine Learning Proceedings 1992*. Elsevier, 1992, pp. 249–256.

[25] S. A. F. Da Silva *et al.*, "Auditory stimulation with music influences the geometric indices of heart rate variability in men," *International archives of medicine*, vol. 7, no. 1, p. 27, 2014.

[26] A. Goshvarpour, A. Abbasi, and A. Goshvarpour, "Gender differences in response to affective audio and visual inductions: Examination of nonlinear dynamics of autonomic signals," *Biom Engin: Applic., Basis and Comm*, vol. 28, no. 04, p. 1650024, 2016.

[27] U. R. Acharya, K. P. Joseph, N. Kannathal, C. M. Lim, and J. S. Suri, "Heart rate variability: a review," *Medical and biological engineering and computing*, vol. 44, no. 12, pp. 1031–1051, 2006.

[28] H. D. Critchley, D. Corfield, M. Chandler, C. Mathias, and R. J. Dolan, "Cerebral correlates of autonomic cardiovascular arousal: a functional neuroimaging investigation in humans," *The Journal of physiology*, vol. 523, no. 1, pp. 259–270, 2000.

[29] M. Brennan, M. Palaniswami, and P. Kamen, "Do existing measures of poincare plot geometry reflect nonlinear features of heart rate variability?" *IEEE transactions on biomedical engineering*, vol. 48, no. 11, pp. 1342–1347, 2001.